

Electronic Supplementary Information

Metal-free generation of hydroxyl radicals by benzoate-mediated decomposition of peroxides

Guoyang Zhang,^a Shuo Lu,^b Chun Zhang,^b Bingdang Wu,^a Yong Liang,^b Zhihao Chen,^a Li Zhang,^a Shujuan Zhang^{*a}

^[a] State Key Laboratory of Pollution Control and Resource Reuse, School of the Environment, Nanjing University, 163 Xianlin Avenue, Nanjing, 210023, China.

^[b] School of Chemistry & Chemical Engineering, Nanjing University, 163 Xianlin Avenue, Nanjing, 210023, China.

*Correspondence author. Phone: +86 25 8968 0389, E-mail: sjzhang@nju.edu.cn

This file includes:

Number of Page: 31

Number of Text: 5

Number of Table: 2

Number of Figure: 14

Number of Chart: 1

Number of Scheme: 2

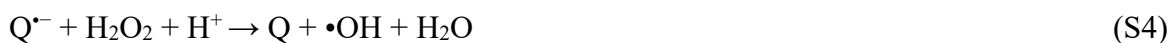
Table of Contents

- Text S1.** The pathways for the production of $\bullet\text{OH}$ from H_2O_2
- Text S2.** Chemicals, analytical methods, and experimental conditions
- Text S3.** Calculation of the quantum yield (Φ) of H_2O_2
- Text S4.** Quantum chemical calculation
- Text S5.** Identification of the 410 nm species
- Table S1.** Analytical conditions for the studied chemicals
- Table S2.** The initial decomposition rates (R_d , $\mu\text{M min}^{-1}$) of BDC and the initial formation rates (R_f , $\mu\text{M min}^{-1}$) of the two hydroxyl products (HBDC and *p*-HBZ) in UV irradiated and N_2 -purged system.
- Fig. S1.** The standard curves for the detection of (a) H_2O_2 with DPD/POD method and (b) PMS with the ABTS method. Scatter: experimental data, line: linear fitting.
- Fig. S2.** The emission spectra of the low-pressure mercury (LP-Hg) lamp.
- Fig. S3.** HPLC profiles of irradiated BDC- H_2O_2 solutions (1–4 min) under N_2 -saturated condition with (a) a UV detector (254 nm) or (b) a fluorescence detector (315_{ex}, 435_{em}).
- Fig. S4.** The formation profiles of the hydroxyl products in the UV irradiated H_2O_2 (40 μM)–BDC (50 μM) solution at air-saturated or N_2 -purged conditions.
- Fig. S5.** The formation profiles of the hydroxyl products in the UV irradiated (a) H_2O_2 (40 μM)–BZ (50 μM) and (b) H_2O_2 (40 μM)–*m*-BDC (50 μM) solution at air-saturated or N_2 -purged conditions.
- Fig. S6.** EPR spectra of UV-irradiated BDC/ H_2O_2 solutions with DMPO (100 mM) as the spin trapping agent. [H_2O_2]: 0.2 mM, [BDC]: 0.2 mM, pH = 9.0, MP-Hg: 0.72 mW cm^{-2} @365 nm, irradiation time: 4 min.
- Fig. S7.** The degradation profiles of COU (50 μM) and the generation profiles of HCOU in UV and UV/ H_2O_2 (40 μM) processes with or without BDC (50 μM) at air-saturated or N_2 -purged conditions. (a) The photodegradation profiles of COU. k_1 (min^{-1}): the pseudo-first-order degradation rate constant. (b) The generation of HCOU. k_0 ($\mu\text{M min}^{-1}$): the pseudo-zero-order formation rate constant.
- Fig. S8.** (a) Left: the decomposition k_1 values of BDC (50 μM) in UV/ H_2O_2 (40 μM) at air-saturated or N_2 -purged conditions. Right: the speciation of BDC at variant pHs.

- Fig. S9.** The decomposition profiles of H_2O_2 (40 μM) in binary mixture with formate (50 μM) at air-saturated or N_2 -purged conditions.
- Fig. S10.** The decomposition profiles of H_2O_2 (20 μM) in H_2O_2 -only or H_2O_2 -BDC (20 μM) binary solutions at air-saturated or O_2 -free conditions (pH: 9.0). The concentration of O_2 in this O_2 -free BDC solution was below the detection limit (0.01 mg L^{-1}). The absorbance of the irradiated solution was controlled below 0.35 to ensure that there was a sufficient number of photons.
- Fig. S11.** Formation of I_3^- in a KI/ KIO_3 chemical actinometer under 254 nm irradiation. $[\text{KI}]_0$: 0.6 M, $[\text{KIO}_3]_0$: 0.1 M, buffer: 10 mM borate, pH 9.0, 25°C. Error bars indicate the standard deviation of duplicate experiments. Scatter: experimental data, line: linear fitting.
- Fig. S12.** Photolysis of a H_2O_2 solution (520 μM) with the LP-Hg lamp. Scatter: experimental data, line: linear fitting.
- Fig. S13.** (a) Transient absorption spectra of BDC at different conditions after laser pulse of 0.2 μs . (b) Decay traces of the 410 nm species. Inset: k_1 of the 410 nm species vs $[\text{H}_2\text{O}_2]_0$ in N_2 -purged BDC solution. $[\text{BDC}]_0$: 0.1 mM, $[\text{KI}]_0$: 0.1 M. MeOH: methanol as the solvent.
- Fig. S14.** Dependence of the 680 nm absorbance (immediately after the 266 nm laser pulse of KI and BDC in N_2 -purged phosphate buffer solutions) on laser intensity. $[\text{BDC}]_0$: 0.5 mM, $[\text{KI}]_0$: 0.251 M, buffer: 20 mM, pH 7.0.
- Chart S1.** Structures and abbreviations of the 16 model compounds.
- Scheme S1.** (a) The energy level diagram of the UV-induced photochemical process in deoxygenated BDC solution with (black) or without (red) H_2O_2 at 298 K. (b) Free energy profile for the subsequent process after the production of BDC^{*+} at 298 K. (c) Free energy profile for the reaction pathway of BDC with $\bullet\text{OH}$ at 298 K.
- Scheme S2.** The possible reaction pathways of $^3\text{BDC}^*$.

Text S1. The pathways for the production of •OH from H₂O₂

There are four well-known pathways for the production of •OH from H₂O₂: UV photolysis (Reaction S1), transition metal-mediated Fenton reactions (Reaction S2), photo-Fenton reactions (Reaction S3), and organic Fenton-like reactions (Reactions S4 and S5).



where M, Q, and X represent metal, quinone and halogen, respectively.

Text S2. Chemicals, analytical methods, and experimental conditions

Chemicals: H₂O₂ of analytical grade was purchased from Shanghai Reagent Station, China. NaOH, KMnO₄, MnSO₄, CoCl₂·6H₂O, HCl, KI, KIO₃, Na₂B₄O₇, NaH₂PO₄·2H₂O and Na₂HPO₄·12H₂O of analytical grade were obtained from Nanjing Reagent Station, China. N, N-diethyl-*p*-phenylenediamine (DPD), sodium thiosulfate (Na₂S₂O₃), peroxymonosulfate (PMS), ammonium molybdate were obtained from Sigma-Aldrich. 5-dimethyl-1-pyrolin-N-oxide (DMPO) of analytical reagent grade was purchased from Dojindo Laboratories Co. Ltd., Japan. Methanol and formic acid of chromatographic grade were purchased from Sigma-Aldrich, China. TBA (99.5%), peroxidase (POD) (≥ 3000 u mg⁻¹) from horseradish were purchased from Shanghai Yuanye Biology Technology Co., Ltd., China. Benzoic acid (99%), *ortho*-hydroxybenzoic acid (99%), *meta*-hydroxybenzoic acid (99%), *para*-hydroxybenzoic acid (99.9%), *ortho*-chlorobenzoic acid (99%), *meta*-chlorobenzoic acid (99%), *para*-chlorobenzoic acid (99%) and ABTS (97%) were purchased from Sigma-Aldrich. Phenol (99%), benzenesulfonic acid (99%) and 2-hydroxyterephthalic acid (98%) were purchased from Aladdin, China. Terephthalic acid (99%) and *para*-hydroxyphenylacetic acid (98%) were purchased from Macklin, China. Phthalic acid (99%), isophthalic acid (99.9%), *ortho*-methylbenzoic acid (99%), *para*-methylbenzoic acid (99%), coumarin (COU, 99%) and 7-hydroxycoumarin (HCOU, 99%) were obtained from J&K, China. High purity N₂ (99.999%) and N₂O (99.95%) were purchased from Nanjing Tianze Gas Co., Ltd., China. Ultrapure water (18.25 MΩ cm) was made by a water purification system (Shanghai Ulupure Industrial Co., Ltd., China) and used for the preparation of sample solutions. Prior to use, 1 g L⁻¹ POD and 10 g L⁻¹ DPD (in 0.05 M H₂SO₄) solutions were prepared and stored in the dark at 4°C. Peracetic acid solution was generated by the reaction between H₂O₂ (30% w/w) and CH₃CO₂H (97% w/w) and stored at 4°C. The titration method was applied to achieve regular calibration.¹

Analytical methods: The O₂-free solutions were prepared in a glove-box system (Mikrouna Co., Ltd., China). UV-Vis spectra were recorded with a double beam spectrophotometer (UV-2700, Shimadzu, Japan). Dissolved oxygen was determined with an HQ30d apparatus (HACH, USA). The concentration of H₂O₂ was determined with the DPD/POD method.² H₂O₂ could oxidize POD to a higher valent state, which in turn oxidized DPD to a pink-colored radical cation DPD⁺ with a

maximum absorption at 551 nm ($\epsilon = 19930 \text{ M}^{-1} \text{ cm}^{-1}$). For the determination of H_2O_2 , an aliquot of 1 mL sample solution was firstly diluted with phosphate buffer (pH 6.0) to 4 mL. And then, 50 μL of DPD (10 g L^{-1} in $0.05 \text{ M H}_2\text{SO}_4$) and 50 μL of POD (1 g L^{-1} in H_2O) were immediately added into the sample. The measurement was finished within $45 \pm 5 \text{ s}$.

The PA solution is a mixture of PA and H_2O_2 (at a molar ratio about 2:3). PA could also oxidize POD. The overall peroxides could be approximately estimated through the DPD/POD method according to the stoichiometric ratio between PA and H_2O_2 .

The concentration of PMS was measured with a colorimetric method.³ Firstly, 1 mL of sample solution was diluted with ultrapure water to 4 mL. Then, 0.2 mL ABTS (10 mM) and 0.2 mL Co^{2+} (10 mM) were added to the solution and let to react for 10 min until the formation of green-colored ABTS radical cations was completed. The resulting solution was analyzed by UV detector at 735 nm. The standard curves for the detection of H_2O_2 (with DPD/POD method) and PMS (with the ABTS method) were showed in Fig. S1.

The concentrations of benzoates were determined with an ultra-high-performance liquid chromatography (UHPLC) system (Dionex U3000, United States). All the tested 18 organic chemicals were analyzed with an Agilent C18 reversed phase column ($150 \text{ mm} \times 4.6 \text{ mm}$, $3.5 \mu\text{m}$) at 25°C and a UV detector. The detection limits were $0.2 \mu\text{M}$ by employing a $50 \mu\text{L}$ injection loop. More details of the UHPLC analysis are listed below. The products of benzoates (BZs) were identified with an LC-MS/MS system in a negative ion mode with an electrospray ionization (ESI) source. An Agilent Eclipse plus C18 column ($150 \text{ mm} \times 4.6 \text{ mm}$, $3.5 \mu\text{m}$) was used for UHPLC separation and the flow rate was 0.2 ml min^{-1} . The settings for ESI were: spray voltage: 3.0 kV, capillary temperature: 350°C , sheath gas flow: 35, auxiliary gas flow: 20 (arbitrary units), capillary voltage: 25 V, and tube lens offset: 100 V.

HPLC profiles of irradiated BDC- H_2O_2 solutions were recorded with a UV detector (254 nm) and a fluorescence detector (315_{ex} , 435_{em}) and are showed in Fig. S3. At the initial stage of the reaction, two product peaks occurred rapidly, which were identified as the hydroxyl products (HBDC and *p*-HBZ) with the LC-MS/MS system. The concentrations of some other possible hydroxyl or decarboxylic products, such as benzoate (BZ), *ortho*-hydroxybenzoate (*o*-HBZ), *meta*-hydroxybenzoate (*m*-HBZ) and phenol (PHE), were below the detection limit ($< 0.2 \mu\text{M}$).

Similar hydroxyl products were also detected in the BZ and *m*-BDC systems and are shown in Fig. S5.

Electron paramagnetic resonance (EPR) spectra were recorded on a Bruker DRX500 spectrometer (Bruker, Germany) with a 180 W a medium-pressure mercury lamp (MP-Hg) for *in situ* irradiation and DMPO as the trapping agent. The running parameters are as follows: center field of 3480.0 G, sweep width of 200 G, microwave frequency of 9.7584 GHz and power of 19.832 mW.

Irradiation experiments: Irradiation experiments were conducted in 50 mL quartz bottles and the temperature was controlled at 25°C. The bottles were placed in a rotating disk photoreactor (PCX-50C, Beijing Perfectlight Co. Ltd.) equipped with nine identical low-pressure mercury lamps (LP-Hg). The LP-Hg lamp has a maximum light emission at 254 nm and a very weak emission at 313 nm (Fig. S2). The light intensity was measured with a radiometer (Photoelectric Instrument Factory of Beijing Normal University, China) equipped with a sensor of peak sensitivity at 254 nm. Prior to irradiation, unless otherwise stated, all the solutions were adjusted with NaOH or HClO₄ solutions to pH 9.0. In purging experiments, the sample solutions were firstly purged with the corresponding gas for 30 min prior to irradiation and then were sealed during UV irradiation.

Laser flash photolysis experiments: Laser flash photolysis experiments were carried out with a LP980 spectrometer from Edinburgh Instruments (UK). The pump source is a Surelite I-10 Q-Switched Nd:YAG laser (35 mJ @266 nm, 100 mJ @355 nm, 120 mJ @532 nm). The repetition rate was 10 Hz. A xenon lamp was employed as the detecting light source. The laser and analyzing light beam passed perpendicularly through a quartz cell with an optical path length of 10 mm. The transient signals of aqueous solutions were recorded with a 100 MHz Tektronix TDS3012C digital oscilloscope and transferred to a computer to analyze the data. The signals were averaged over ten to twenty laser shots to improve the signal-to-noise ratio. All components are controlled by the software L900 provided by Edinburgh.

Text S3. Calculation of the quantum yield (Φ) of H_2O_2

The quantum yield ($\Phi_{\text{H}_2\text{O}_2}^{\text{BZs}}$) of H_2O_2 in the deoxygenated benzoates (BZs)/ H_2O_2 solution under UV irradiation is defined as the moles of H_2O_2 come exclusively from the BZs-mediated decomposition divided by the moles of photons absorbed by BZs in BZs– H_2O_2 mixed solution. As shown in equation S6, the photodecomposition of H_2O_2 in BZs– H_2O_2 binary solution was composed of the direct photolysis of H_2O_2 ($I_{\text{H}_2\text{O}_2} \Phi_{\text{H}_2\text{O}_2}^{\text{blank}}$) and the BZs-mediated decomposition ($I_{\text{BZs}} \Phi_{\text{H}_2\text{O}_2}^{\text{BZs}}$).

$$\frac{dC_t}{dt} = I_{\text{H}_2\text{O}_2} \Phi_{\text{H}_2\text{O}_2}^{\text{blank}} + I_{\text{BZs}} \Phi_{\text{H}_2\text{O}_2}^{\text{BZs}} \quad (\text{S6})$$

where C_t is the concentration of H_2O_2 (M), $I_{\text{H}_2\text{O}_2}$ and I_{BZs} (einstein s^{-1}) are the number of absorbed photons per unit time for H_2O_2 and benzoates (BZs) in the binary solution, respectively, which are related to the absorption coefficients ($\epsilon_{254 \text{ nm}}$) and are suffered from inner filter effect, i.e., the competition for photons between H_2O_2 and BZs. $\Phi_{\text{H}_2\text{O}_2}^{\text{blank}}$ and $\Phi_{\text{H}_2\text{O}_2}^{\text{BZs}}$ are the quantum yields of the direct photolysis of H_2O_2 ($\Phi_{\text{H}_2\text{O}_2}^{\text{blank}} = 0.5$)⁴ and the benzoates-mediated decomposition, respectively.

$I_{\text{H}_2\text{O}_2}$ and I_{BZs} could be calculated with the following equations:⁵

$$I_{\text{H}_2\text{O}_2} = \frac{\alpha_{\text{H}_2\text{O}_2} \times I_0 \times (1 - 10^{(-\alpha_{\text{tot}} \times L)})}{\alpha_{\text{tot}}} \quad (\text{S7})$$

$$I_{\text{BZs}} = \frac{\alpha_{\text{BZs}} \times I_0 \times (1 - 10^{(-\alpha_{\text{tot}} \times L)})}{\alpha_{\text{tot}}} \quad (\text{S8})$$

where I_0 is the photon flux entering the solution (einstein s^{-1}), α_{tot} (cm^{-1}) is the total absorbance of the BZs– H_2O_2 solution, $\alpha_{\text{H}_2\text{O}_2}$ and α_{BZs} (cm^{-1}) are the absorbances of H_2O_2 and BZs, respectively. L is the effective path length (cm).

Accordingly, $\Phi_{\text{H}_2\text{O}_2}^{\text{BZs}}$, can be calculated as follows:

$$\begin{aligned} \Phi_{\text{H}_2\text{O}_2}^{\text{BZs}} &= \frac{r_0 V - I_{\text{H}_2\text{O}_2} \Phi_{\text{H}_2\text{O}_2}^{\text{blank}}}{I_{\text{BZs}}} \\ &= \frac{\alpha_{\text{tot}} r_0 V - \alpha_{\text{H}_2\text{O}_2} \times I_0 \times (1 - 10^{(-\alpha_{\text{tot}} \times L)}) \times \Phi_{\text{H}_2\text{O}_2}^{\text{blank}}}{\alpha_{\text{BZs}} \times I_0 \times (1 - 10^{(-\alpha_{\text{tot}} \times L)})} \end{aligned} \quad (\text{S9})$$

where r_0 is the decomposition rate of H_2O_2 (M s^{-1}), V is the solution volume (L).

The I_0 (einstein s^{-1}) entering the solution from the LP-Hg lamp was determined by the method of KI/KIO₃ method.^{6,7} A solution of 0.6 M KI and 0.1 M KIO₃ in 0.01 M borate buffer (pH 9.0) was selected as the chemical actinometer. The photons entering the solution were assumed to be totally absorbed by the optically opaque solution. The irradiation of the chemical actinometer led to the formation of I_3^- and the concentration of I_3^- was quantified with the absorbance at 352 nm and a molar extinction coefficient of $26400 \text{ M}^{-1} \text{ cm}^{-1}$.

$$I_0 = C_{\text{tri}} \times V \times \frac{1}{\Phi_{\text{tri}}} \times \frac{1}{t} \quad (\text{S10})$$

where C_{tri} is concentration of I_3^- (M), V is solution volume (L), Φ_{tri} is quantum yield of I_3^- (moles/einstein), and t is time (s). At 25°C, $\Phi_{\text{tri}} = 0.82$ moles/einstein, $V = 25$ mL, the I_0 was calculated as $2.56 \pm 0.04 \times 10^{-8}$ einstein s^{-1} from the slope in Fig. S11.

The L was determined by photolysis of a H_2O_2 solution.⁸ When total absorbance of H_2O_2 is low, its photolysis approximately follows the first-order kinetic model:⁹

$$\frac{dC_t}{dt} = \left(\frac{-2.303\varepsilon_1 L I_0 \Phi_{\text{total}}}{V} \right) \times C_t \quad (\text{S11})$$

where C_t is the concentration of H_2O_2 (M), ε_1 is the molar absorption coefficient of H_2O_2 ($\text{M}^{-1} \text{ cm}^{-1}$), Φ_{total} is the total quantum yield for H_2O_2 photolysis (moles/einstein). At 254 nm, $\varepsilon_1 = 19.6 \text{ M}^{-1} \text{ cm}^{-1}$, $\Phi_{\text{total}} = 1.0$,¹⁰ $I_0 = 2.56 \pm 0.04 \times 10^{-8}$ einstein s^{-1} . L was calculated as 3.16 ± 0.05 cm from the slope in Fig. S12. The obtained L was close to the physical optical path (3.43 cm).

Text S4. Quantum chemical calculation

All the calculations were performed with the density functional theory (DFT) and time-dependent density functional theory (TD-DFT) using the Gaussian 09 software package.¹¹ Geometry optimizations of the reactants, transition states (TS), intermediates (Int) and products were conducted at the B3LYP/6-31+G(d) level of theory in water followed by frequency calculations to evaluate zero-point vibrational energies (ZPVE) and thermal corrections at 298 K. The energies of the species after optimization were calculated at the B3LYP-D3/6-311+G(d,p) level of theory in water.¹² The solvent effect of water was considered based on the CPCM model.¹³ Intrinsic reaction coordinate (IRC) analysis was executed to ensure that each TS uniquely connected the designated reactants with the products.

Below are the energies and Cartesian coordinates obtained from DFT calculation:

BDC

$G(\text{water}) = -608.6185648$ Hartree

```
-----  
C  0.698352 -1.203701  0.000000  
C  1.420907  0.000019  0.000000  
C  0.698327  1.203723  0.000000  
C -0.698352  1.203701  0.000000  
C -1.420907 -0.000019  0.000000  
C -0.698327 -1.203724  0.000000  
H  1.245837 -2.141422  0.000000  
H  1.245780  2.141459  0.000000  
H -1.245837  2.141421  0.000000  
H -1.245780 -2.141460  0.000000  
C  2.952171 -0.000042  0.000000  
O  3.528897  1.128097 -0.000001  
O  3.528812 -1.128097  0.000001  
C -2.952170  0.000042  0.000000  
O -3.528897 -1.128097 -0.000001  
O -3.528812  1.128099  0.000001  
-----
```

¹BDC*

$G(\text{water}) = -608.4970595$ Hartree

```
-----  
C  0.700911  1.214633 -0.000022  
C  1.449121  0.000000 -0.000020  
C  0.700909 -1.214633 -0.000021  
C -0.679402 -1.229357 -0.000016  
C -1.429192  0.000002 -0.000009  
C -0.679400  1.229359 -0.000017  
H  1.247614  2.153693 -0.000032  
H  1.247611 -2.153694 -0.000030  
H -1.212544 -2.177625 -0.000019  
H -1.212541  2.177628 -0.000021  
C  2.943545 -0.000001 -0.000011  
O  3.547054 -1.129396  0.000040  
O  3.547054  1.129395  0.000041  
C -2.839816  0.000002  0.000018  
O -3.613942  1.044408  0.000008  
O -3.613940 -1.044411 -0.000002  
-----
```

³BDC* $G(\text{water}) = -608.511918219$ Hartree

```

-----
C  0.680069 -1.242533  0.185987
C  1.448158 -0.000002  0.000015
C  0.680071  1.242530 -0.185964
C -0.680070  1.242530 -0.185968
C -1.448158 -0.000001  0.000004
C -0.680071 -1.242533  0.185982
H  1.237947 -2.161827  0.334877
H  1.237950  2.161823 -0.334852
H -1.237947  2.161823 -0.334862
H -1.237950 -2.161826  0.334868
C  2.930009 -0.000002  0.000021
O  3.520106  1.111852  0.214699
O  3.520110 -1.111833 -0.214766
C -2.930009 -0.000002 -0.000001
O -3.520105 -1.111845 -0.214739
O -3.520108  1.111847  0.214697
-----

```

BDC⁺ $G(\text{water}) = -608.4090015$ Hartree

```

-----
C -0.691308 -1.225489  0.006046
C  0.691033 -1.225331 -0.004511
C  1.402793  0.000182 -0.000093
C  0.690800  1.225553  0.004333
C -0.691545  1.225441 -0.006220
C -1.402556 -0.000092 -0.000082
H -1.242403 -2.160896  0.016644
H  1.242339 -2.160596 -0.013880
H  1.241928  2.160923  0.013686
H -1.242819  2.160741 -0.016798
-----

```

```

C -2.900503 -0.000289 -0.000085
O -3.474285 -0.582338  0.957301
O -3.474450  0.582371 -0.956996
C  2.899720  0.000323 -0.000134
O  3.475010  0.586487  0.954363
O  3.475018 -0.586764 -0.954065
-----

```

TS1 $G(\text{water}) = -608.3908837$ Hartree

```

-----
C -0.743667  1.209522 -0.000030
C  0.660560  1.231900 -0.000033
C  1.279341 -0.000006 -0.000023
C  0.660548 -1.231902  0.000018
C -0.743679 -1.209501  0.000026
C -1.453915  0.000016  0.000005
H -1.292643  2.146031 -0.000050
H  1.214789  2.163321 -0.000050
H  1.214764 -2.163330  0.000035
H -1.292668 -2.146003  0.000054
C -2.989983 -0.000001  0.000006
O -3.557908  1.129504  0.000158
O -3.557868 -1.129528 -0.000152
C  3.296843 -0.000002  0.000009
O  3.580375 -1.164113  0.000093
O  3.580336  1.164116 -0.000080
-----

```

BZ⁺ $G(\text{water}) = -419.7569828$ Hartree

```

-----
C  0.000068 -1.904696  1.227251
-----

```

C -0.000047 -0.498793 1.211100
 C -0.000537 0.212373 0.000000
 C -0.000047 -0.498793 -1.211100
 C 0.000068 -1.904696 -1.227251
 C 0.000135 -2.536148 0.000000
 H 0.000178 -2.451243 2.167085
 H 0.000079 0.054769 2.145380
 H 0.000079 0.054769 -2.145380
 H 0.000178 -2.451243 -2.167085
 C 0.000095 1.745578 0.000000
 O 0.000068 2.318999 -1.128560
 O 0.000068 2.318999 1.128560

TS2

$G(\text{water}) = -496.1980394$ Hartree

C 1.212068 -1.222340 -0.037546
 C -0.189962 -1.209089 -0.018422
 C -0.901887 -0.000002 -0.007935
 C -0.189963 1.209084 -0.018532
 C 1.212067 1.222333 -0.037670
 C 1.869830 -0.000004 -0.057992
 H 1.758253 -2.161481 -0.042830
 H -0.740744 -2.144430 -0.009668
 H -0.740749 2.144423 -0.009851
 H 1.758255 2.161472 -0.043052
 C -2.436663 0.000002 0.018727
 O -3.007697 1.128914 0.028800
 O -3.007712 -1.128905 0.028502
 O 4.378606 0.000019 -0.026733
 H 4.482453 -0.000107 0.946311
 H 3.124011 0.000002 -0.129228

TS3

$G(\text{water}) = -571.3443701$ Hartree

C 0.000068 -1.904696 1.227251
 C -0.000047 -0.498793 1.211100
 C -0.000537 0.212373 0.000000
 C -0.000047 -0.498793 -1.211100
 C 0.000068 -1.904696 -1.227251
 C 0.000135 -2.536148 0.000000
 H 0.000178 -2.451243 2.167085
 H 0.000079 0.054769 2.145380
 H 0.000079 0.054769 -2.145380
 H 0.000178 -2.451243 -2.167085
 C 0.000095 1.745578 0.000000
 O 0.000068 2.318999 -1.128560
 O 0.000068 2.318999 1.128560

BZ

$G(\text{water}) = -420.4321507$ Hartree

C -0.272702 -0.899870 -0.000011
 C 1.126889 -0.917263 0.000580
 C 1.842681 0.283839 0.000137
 C 1.176484 1.519419 -0.000854
 C -0.227182 1.524215 -0.001416
 C -0.948275 0.326081 -0.001022
 H -0.831435 -1.832705 0.000310
 H 1.659543 -1.865551 0.001368
 H 2.928218 0.277286 0.000554
 H -0.745639 2.478027 -0.002171

H -2.035689 0.347891 -0.001492
C 1.966836 2.832458 -0.001329
O 1.299238 3.908537 -0.002053
O 3.229808 2.740257 -0.000936

***p*-HBZ**

$G(\text{water}) = -495.6829917$ Hartree

C 1.426590 1.157998 0.106564
C 0.031086 1.187007 0.054874
C -0.724288 0.006325 -0.000564
C -0.032797 -1.216423 -0.001780
C 1.359977 -1.265633 0.050661
C 2.092718 -0.073645 0.104596
H 1.994382 2.085630 0.147598
H -0.487969 2.140327 0.056654
H -0.603355 -2.138785 -0.044876
H 1.887949 -2.215596 0.049753
C -2.249437 0.049698 -0.059096
O -2.856440 -1.060735 -0.131446
O -2.796567 1.192779 -0.031180
O 3.461574 -0.174270 0.154038
H 3.860409 0.711062 0.187274

Int1

$G(\text{water}) = -684.3957276$ Hartree

C -0.171344 -1.125641 -0.000737
C 1.223418 -1.193591 0.001354
C 2.003289 -0.026385 0.000098
C 1.342446 1.212258 -0.003540

C -0.051806 1.282163 -0.005395
C -0.829917 0.114027 -0.004033
H -0.763964 -2.035180 0.000557
H 1.724799 -2.156567 0.004161
H 1.936159 2.121105 -0.004890
H -0.552870 2.245464 -0.007950
C 3.533724 -0.100968 0.003044
O 4.054067 -1.255583 -0.000845
O 4.162109 0.998489 0.009346
C -2.348796 0.196009 -0.005717
O -2.886318 1.335930 -0.000272
O -2.986780 -0.910898 -0.012522
O -5.588419 -0.383091 0.016927
H -4.587494 -0.600832 -0.003393

TS4

$G(\text{water}) = -684.388901$ Hartree

C 0.769851 0.978663 -0.455519
C -0.650258 0.960264 -0.427522
C -1.341271 -0.252769 -0.138701
C -0.589903 -1.370604 0.218586
C 0.812265 -1.323697 0.232660
C 1.511271 -0.149337 -0.110044
H 1.288492 1.892699 -0.724366
H -1.208803 1.771922 -0.874912
H -1.107212 -2.291020 0.470830
H 1.385076 -2.205626 0.502086
C -2.866155 -0.316130 -0.231793
O -3.438232 0.635684 -0.838618
O -3.429505 -1.319485 0.294313
C 3.043274 -0.121225 -0.116180

O 3.633899 -1.202015 0.174809
O 3.594126 0.978497 -0.412593
O -0.883754 2.025374 1.390105
H -0.304278 1.456599 1.933302

Int2

G(water) = -684.4072465 Hartree

C 1.341538 -0.256010 -0.038665
C 0.676077 1.089071 -0.139421
C -0.821510 1.029985 -0.229169
C -1.540890 -0.123087 -0.053044
C -0.838574 -1.347156 0.159771
C 0.573042 -1.385337 0.149510
H -1.347541 1.967403 -0.391001
H -1.410890 -2.256989 0.304400
H 1.079799 -2.340405 0.261905
C -3.074777 -0.112615 -0.094753
O -3.655747 -1.226390 0.067359
O -3.643102 1.001684 -0.288081
C 2.848370 -0.344645 -0.192560
O 3.430067 -1.351536 0.314051
O 3.410978 0.588648 -0.842962
O 1.053869 1.851101 1.067714
H 0.835195 2.785014 0.904999
H 1.095254 1.635684 -0.994969

TS5

G(water) = -760.1810646 Hartree

C -1.079358 -0.594660 -0.055269

C -0.542726 0.817127 -0.203320
C 0.948519 0.942766 -0.133941
C 1.768568 -0.139720 0.003263
C 1.198211 -1.453511 0.105927
C -0.196680 -1.647488 0.061705
H 1.368889 1.939970 -0.219339
H 1.866360 -2.299929 0.216785
H -0.600655 -2.654397 0.131129
C 3.295399 0.037530 0.062329
O 3.968294 -0.994790 0.348859
O 3.753053 1.191551 -0.172630
C -2.573441 -0.781126 -0.105875
O -3.063644 -1.917559 0.103089
O -3.249110 0.284961 -0.373960
O -1.021569 1.426635 -1.396256
H -1.992181 1.227273 -1.368408
H -0.994230 1.443415 0.672124
O -2.109174 1.977219 1.627250
H -2.781924 1.514020 1.067974

HBDC

G(water) = -683.8808602 Hartree

C 0.772168 1.038208 0.000017
C -0.628821 0.966781 0.000011
C -1.281001 -0.291304 -0.000016
C -0.479488 -1.444999 -0.000040
C 0.911037 -1.372690 -0.000038
C 1.553408 -0.120268 -0.000007
H 1.252435 2.011577 0.000035
H -0.979405 -2.409478 -0.000057
H 1.512747 -2.275370 -0.000054

C	-2.793230	-0.395070	-0.000002
O	-3.329344	-1.530252	-0.000009
O	-3.439920	0.719150	0.000022
C	3.084456	-0.023404	0.000001
O	3.726815	-1.114775	0.000119
O	3.590956	1.137194	-0.000101
O	-1.337353	2.127250	0.000029
H	-2.306182	1.821212	0.000034

H₂O

G(water) = -76.46303301 Hartree

O	0.000000	0.000000	0.118603
H	0.000000	0.768372	-0.474413
H	0.000000	-0.768372	-0.474413

H₂O^{•-}

G(water) = -76.48045461 Hartree

O	0.000000	0.129715	0.0000007
H	0.773669	-0.518888	0.0000005
H	-0.773669	-0.518833	0.0000004

H₂O₂

G(water) = -151.6066638 Hartree

O	-0.820544	-2.708227	-0.402215
---	-----------	-----------	-----------

H	-0.140427	-2.331434	0.187447
O	-1.816050	-1.649417	-0.402214
H	-2.496174	-2.026218	0.187434

H₂O₂^{•-}

G(water) = -151.7615479 Hartree

O	-1.135511	-0.087581	-0.028012
H	-0.954991	0.833112	0.224094
O	1.135516	0.087580	-0.028012
H	0.954949	-0.833103	0.224098

CO₂

G(water) = -188.6589444 Hartree

C	0.000000	0.000000	0.0000002
O	0.000000	0.000000	1.1691324
O	0.000000	0.000000	-1.1691322

OH[•]

G(water) = -75.77617526 Hartree

O	0.000000	0.000000	0.109334
H	0.000000	0.000000	-0.874669

Text S5. Identification of the 410 nm species

It is reported that several transient species of benzoquinone, such as semiquinone radical, radical ion, and OH-adduct, might have absorption at 410 nm.¹⁴ Similarly, various transient species, including BDC radical cation ($\text{BDC}^{\bullet+}$) from the photoionization of BDC, BDC radical anion ($\text{BDC}^{\bullet-}$) from the reaction of $e_{\text{aq}}^{\bullet-}$ with BDC, $\bullet\text{H-BDC}$ from the reaction of ${}^3\text{BDC}^*$ with H_2O , and OH-adduct of BDC ($\bullet\text{OH-BDC}$) from either the addition of free $\bullet\text{OH}$ to BDC or the further evolution of $\text{BDC}^{\bullet+}$ (Scheme S2), might be attributable to the 410 nm species.

In order to clarify the attribution of the 410 nm species, a series of trapped experiments were conducted, including (1) purging the solution with N_2O to convert hydrated electron ($e_{\text{aq}}^{\bullet-}$) to $\bullet\text{OH}$ (Reaction S12).¹⁵ In this way, the 410 nm peak might be enhanced if the species was $\bullet\text{OH-BDC}$ or disappeared if it was from $\text{BDC}^{\bullet-}$; (2) adding KI to the BDC solution to purposely generate more $e_{\text{aq}}^{\bullet-}$ (Reaction S13)¹⁶ to see whether the 410 nm species was $\text{BDC}^{\bullet-}$; (3) replacing water with a better hydrogen donor/ $\bullet\text{OH}$ scavenger, methanol, as the solvent to check whether the 410 nm species was $\bullet\text{H-BDC}$ or $\bullet\text{OH-BDC}$; (4) dosing H_2O_2 to purposely generate $\bullet\text{OH}$ (Reaction S1) to check whether the 410 nm species was $\bullet\text{OH-BDC}$.



As shown in Fig. S13, the 410 nm peak was nearly unaffected by N_2O -purging, excluding the possibility that the 410 nm peak was from $\text{BDC}^{\bullet-}$. The photolysis of KI generated I_2^- and $e_{\text{aq}}^{\bullet-}$, leading to two broad absorption peaks at 390 nm and 680 nm, respectively. The 320 nm peak in the BDC solution was shifted to 360 nm by the addition of KI, which might be due to the formation of complexes between ${}^3\text{BDC}^*$ and I_2^- . A new peak appeared at 530 nm in the BDC/KI solution, which should be from the reaction product of $e_{\text{aq}}^{\bullet-}$ with BDC ($\text{BDC}^{\bullet-}$). Based on the N_2O -purging and KI-dosing results, it is reasonable to infer that the 410 nm peak was not attributable to $\text{BDC}^{\bullet-}$. With methanol as the solvent, the 410 nm peak disappeared, indicating that the 410 nm species was not $\bullet\text{H-BDC}$. The possibility of the 410 nm species as $\bullet\text{OH-BDC}$ was excluded by the H_2O_2 -dosing experiments, in which the decay k_1 of the 410 nm species was positively related to the

concentration of H₂O₂, demonstrating that the 410 nm species was not •OH-BDC. Therefore, we believe that it is reasonable to infer the 410 nm species to BDC⁺.

References

1. Y. Wang, J. Le Roux, T. Zhang and J. P. Croué, *Environ. Sci. Technol.*, 2014, **48**, 14534–14542.
2. H. Bader, V. Sturzenegger and J. Hoigne, *Water Res.*, 1988, **22**, 1109–1115.
3. P. Sun, T. Zhang, B. Mejia-Tickner, R. Zhang, M. Cai and C. H. Huang, *Environ. Sci. Technol. Lett.*, 2018, **5**, 400–404.
4. R. Zellner, M. Exner and H. Herrmann, *J. Atmos. Chem.*, 1990, **10**, 411–425.
5. B. D. Wu, M. H. Yang, R. Yin, S. J. Zhang, *J. Hazard. Mater.*, 2017, **335**, 100–107.
6. R. O. Rahn, *Photochem. Photobiol.*, 1997, **66**, 450–455.
7. X. C. Li, J. Ma, G. F. Liu, J. Y. Fang, S. Y. Yue, Y. H. Guan, L. W. Chen and X. W. Liu, *Environ. Sci. Technol.*, 2012, **46**, 7342–7349.
8. F. J. Beltran, G. Ovejero, J. F. Garcia-Araya and J. Rivas, *Ind. Eng. Chem. Res.*, 1995, **34**, 1607–1615.
9. J. C. Crittenden, S. M. Hu, D. W. Hand and S. A. Green, *Water Res.*, 1999, **33**, 2315–2328.
10. J. H. Baxendale and J. A. Wilson, *Trans. Faraday Soc.*, 1957, **53**, 344–356.
11. M. J. T. Frisch, G. W. Trucks, H. B. Schlegel, G. E. Scuseria, M. A. Robb, J. R. Cheeseman, G. Scalmani, V. Barone, B. Mennucci, G. A. Petersson, H. Nakatsuji, M. Caricato, X. Li, H. P. Hratchian, A. F. Izmaylov, J. Bloino, G. Zheng, J. L. Sonnenberg, M. Hada, M. Ehara, K. Toyota, R. Fukuda, J. Hasegawa, M. Ishida, T. Nakajima, Y. Honda, O. Kitao, H. Nakai, T. Vreven, J. A. Montgomery, J. E. Jr Peralta, F. Ogliaro, M. Bearpark, J. J. Heyd, E. Brothers, K. N. Kudin, V. N. Staroverov, R. Kobayashi, J. Normand, K. Raghavachari, A. Rendell, J. C. Burant, S. S. Iyengar, J. Tomasi, M. Cossi, N. Rega, J. M. Millam, M. Klene, J. E. Knox, J. B. Cross, V. Bakken, C. Adamo, J. Jaramillo, R. Gomperts, R. E. Stratmann, O. Yazyev, A. J. Austin, R. Cammi, C. Pomelli, J. W. Ochterski, R. L. Martin, K. Morokuma, V. G. Zakrzewski, G. A. Voth, P. Salvador, J. J. Dannenberg, S. Dapprich, A. D. Daniels, O. Farkas, J. B. Foresman, J. V. Ortiz, J. Cioslowski, D. J. Fox, **2010**. Gaussian 09, Revision E.01, Gaussian, Inc.: Wallingford CT.
12. C. Lee, W. Yang and R. G. Parr, *Phys. Rev. B*, 1988, **37**, 785–789.

13. M. Cossi, N. Rega, G. Scalmani and V. Barone, *J. Comput. Chem.*, 2003, **24**, 669–681.
14. G. E. Adams and B. D. Michael, *Trans. Faraday Soc.*, 1967, **63**, 1171–1180.
15. G. V. Buxton, C. L. Greenstock, W. P. Helman and A. B. Ross, *J. Phys. Chem. Ref. Data*, 1988, **17**, 513–886.
16. C. D. Borsarelli, S. G. Bertolotti and C. M. Previtali, *Photochem. Photobiol. Sci.*, 2003, **2**, 791–795.

Table S1. Analytical conditions for the studied chemicals

Chemical	Eluent (v/v %)	Flow rate (mL min ⁻¹)	λ (nm)	Retention time (min)
BZ	60 ^a : 40 ^b	0.30	225	7.2
PHE	60 : 40	0.30	210	6.0
BS	40 : 60	0.30	210	4.3
<i>p</i> -HPA	40 : 60	0.30	221	5.3
COU	60 : 40	0.30	278	6.2
HCOU	60 : 40	0.30	332 _{ex} , 471 _{em} ^c	5.3
<i>o</i> -HBZ	60 : 40	0.30	315 _{ex} , 435 _{em}	8.7
<i>m</i> -HBZ	60 : 40	0.30	210	4.8
<i>p</i> -HBZ	60 : 40	0.30	210	4.5
<i>o</i> -BDC	60 : 40	0.30	254	4.3
<i>m</i> -BDC	60 : 40	0.30	254	5.3
BDC	60 : 40	0.30	254	5.0
HBDC	60 : 40	0.30	315 _{ex} , 435 _{em}	5.1
<i>o</i> -CBZ	70 : 30	0.50	210	7.4
<i>m</i> -CBZ	70 : 30	0.50	234	4.8
<i>p</i> -CBZ	70 : 30	0.50	234	4.9
<i>o</i> -MBZ	70 : 30	0.50	210	4.0
<i>p</i> -MBZ	70 : 30	0.50	234	4.0

^a methanol, ^b (0.1%) formic acid solution, ^c ‘ex’ and ‘em’ represents excitation and emission.

Table S2. The initial decomposition rates (R_d , $\mu\text{M min}^{-1}$) of BDC and the initial formation rates (R_f , $\mu\text{M min}^{-1}$) of the two hydroxyl products (HBDC and *p*-HBZ) in UV irradiated and N₂-purged system.

	UV	UV/H ₂ O ₂	UV/H ₂ O ₂ /TBA	Inhibition ^b
R_d , BDC	0.188	16.532	6.310	61.8%
R_f , HBDC	0.025	3.156	1.260	60.1%
R_f , <i>p</i> -HBZ	Nd ^a	1.648	0.610	63.0%

^a Not detectable (the detection limits of HBDC and *p*-HBZ were 0.001 μM and 0.2 μM , respectively). ^b Inhibition rate caused by TBA: $1 - R_{w/TBA}/R_{w/o\ TBA}$. [TBA]₀: 100 mM, [BDC]₀: 50 μM , [H₂O₂]₀: 40 μM .

Supplementary Figures

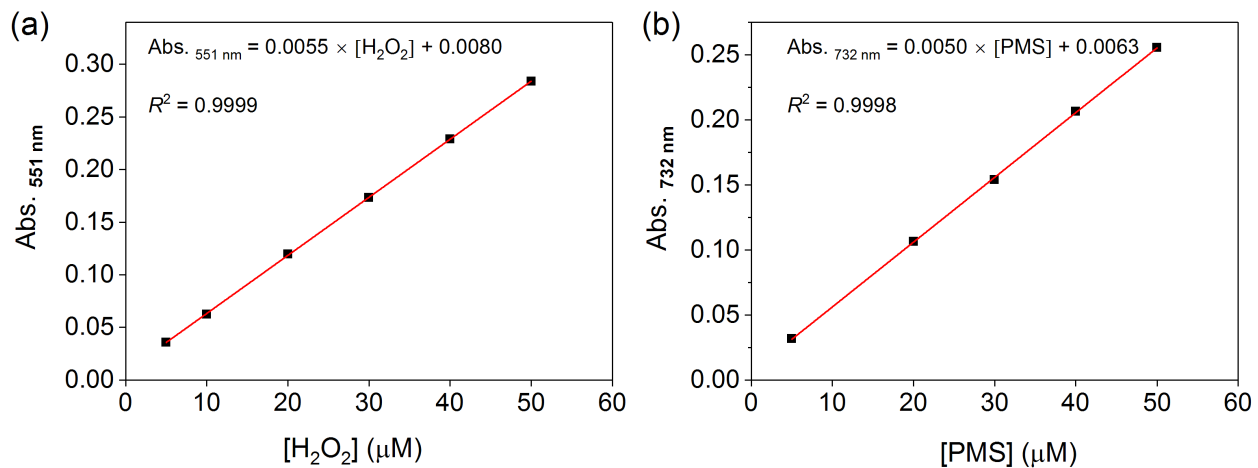


Fig. S1. The standard curves for the detection of (a) H₂O₂ with DPD/POD method and (b) PMS with the ABTS method. Scatter: experimental data, line: linear fitting.

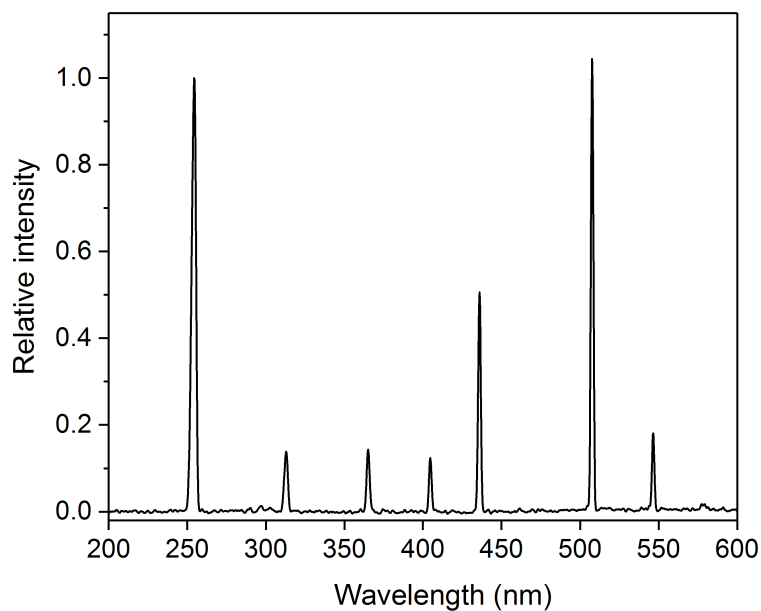


Fig. S2. The emission spectra of the low-pressure mercury (LP-Hg) lamp.

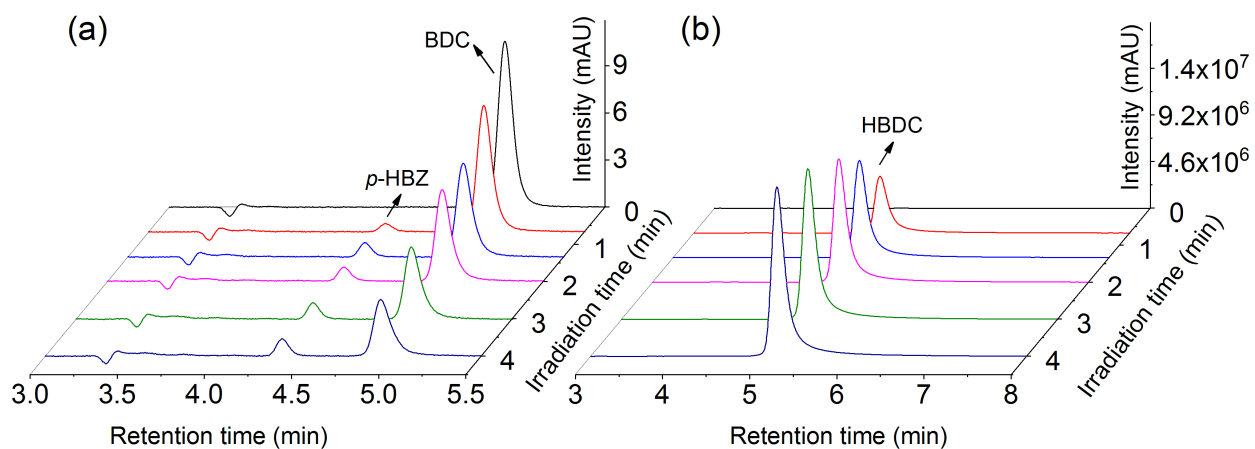


Fig. S3. HPLC profiles of irradiated BDC–H₂O₂ solutions (1–4 min) under N₂-saturated condition with (a) a UV detector (254 nm) or (b) a fluorescence detector (315_{ex}, 435_{em}).

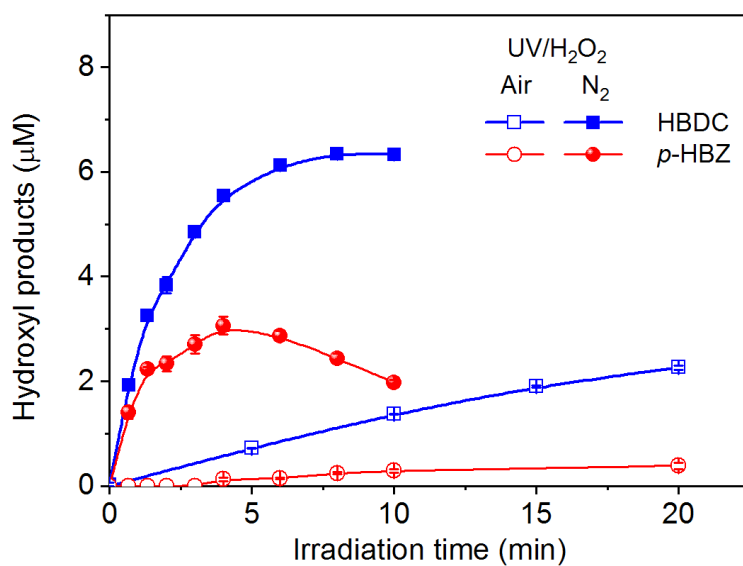


Fig. S4. The formation profiles of the hydroxyl products in the UV irradiated H₂O₂ (40 μM)–BDC (50 μM) solution at air-saturated or N₂-purged conditions.

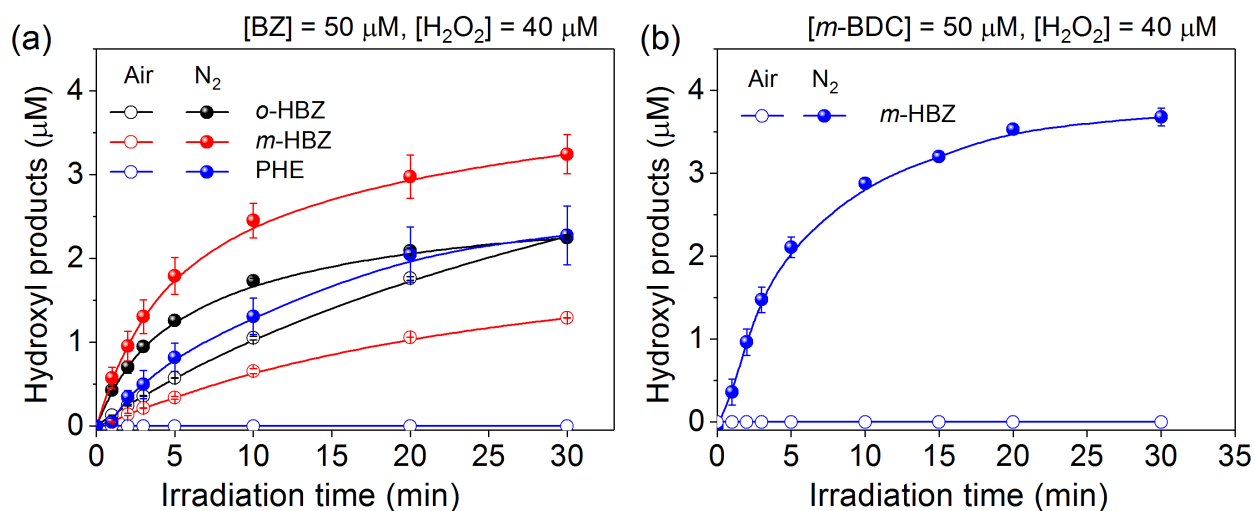


Fig. S5. The formation profiles of the hydroxyl products in the UV irradiated (a) H₂O₂ (40 μM)–BZ (50 μM) and (b) H₂O₂ (40 μM)–*m*-BDC (50 μM) solution at air-saturated or N₂-purged conditions.

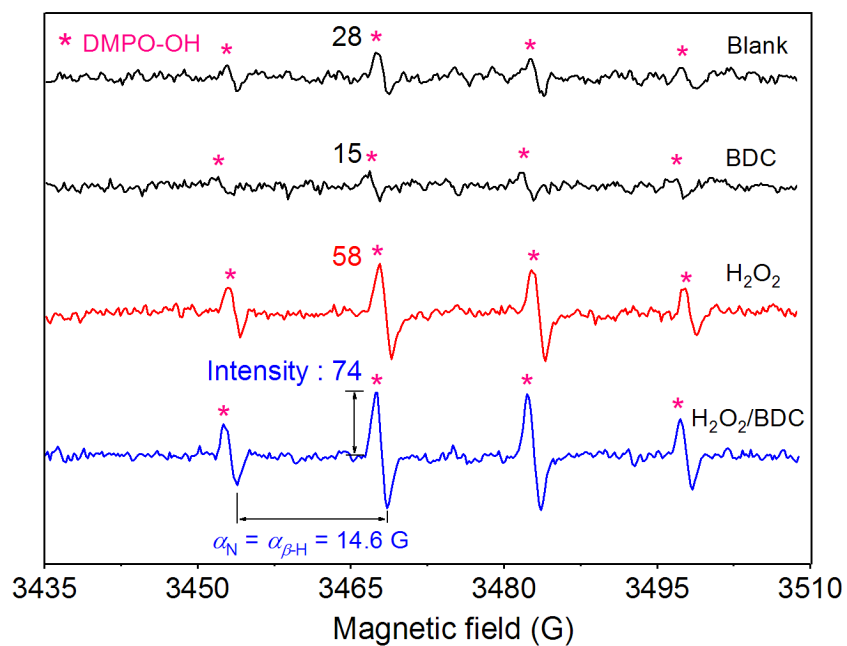


Fig. S6. EPR spectra of UV-irradiated BDC/H₂O₂ solutions with DMPO (100 mM) as the spin trapping agent. [H₂O₂]: 0.2 mM, [BDC]: 0.2 mM, pH = 9.0, MP-Hg: 0.72 mW cm⁻² @365 nm, irradiation time: 4 min.

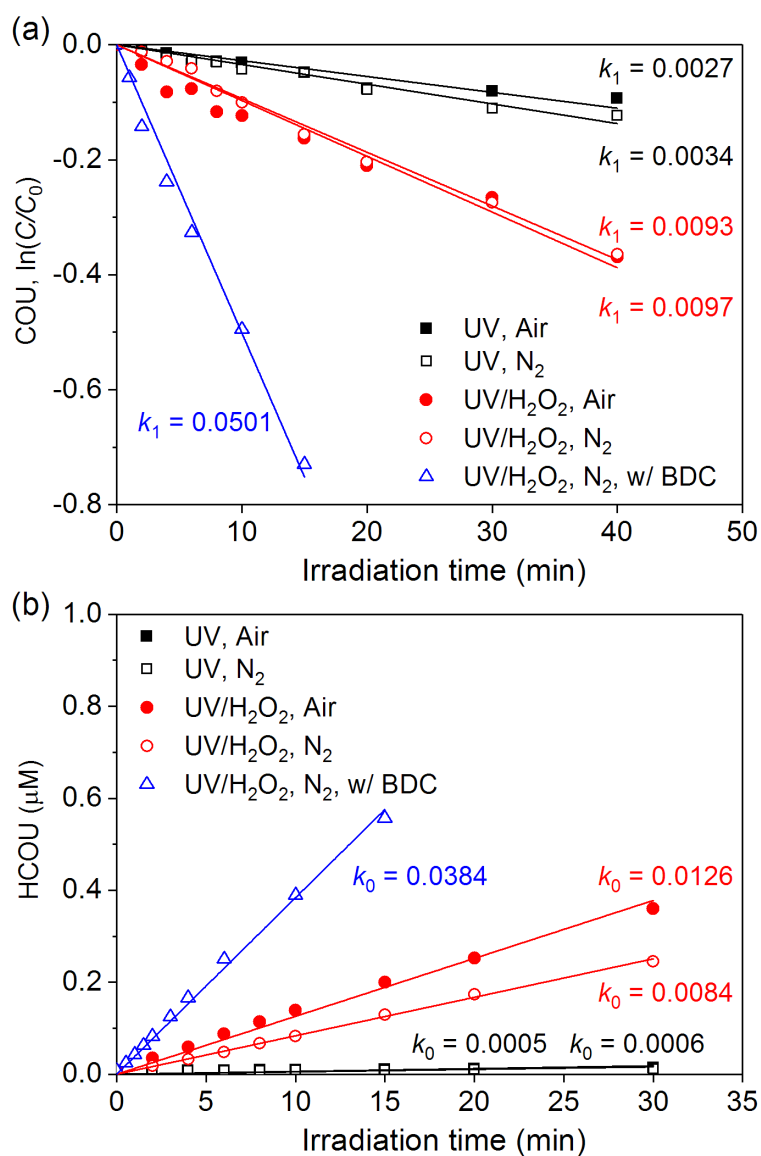


Fig. S7. The degradation profiles of COU (50 μM) and the generation profiles of HCOU in UV and UV/ H_2O_2 (40 μM) processes with or without BDC (50 μM) at air-saturated or N_2 -purged conditions. (a) The photodegradation profiles of COU. k_1 (min^{-1}): the pseudo-first-order degradation rate constant. (b) The generation of HCOU. k_0 ($\mu\text{M min}^{-1}$): the pseudo-zero-order formation rate constant.

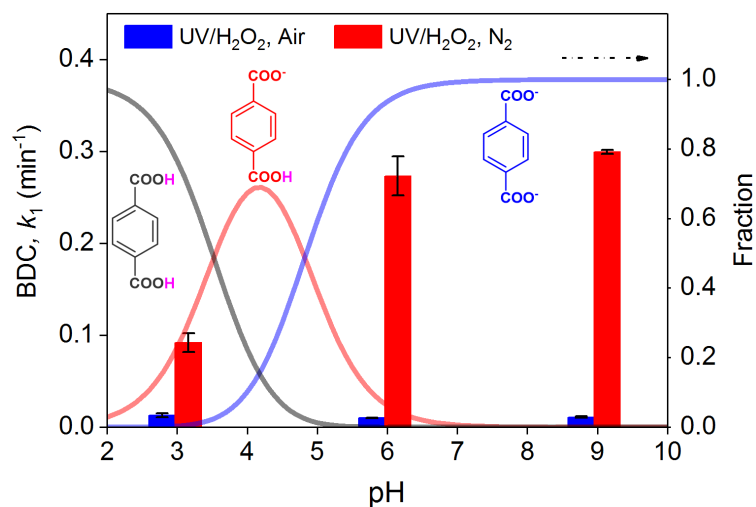


Fig. S8. (a) Left: the decomposition k_1 values of BDC (50 μM) in UV/H₂O₂ (40 μM) at air-saturated or N₂-purged conditions. Right: the speciation of BDC at variant pHs.

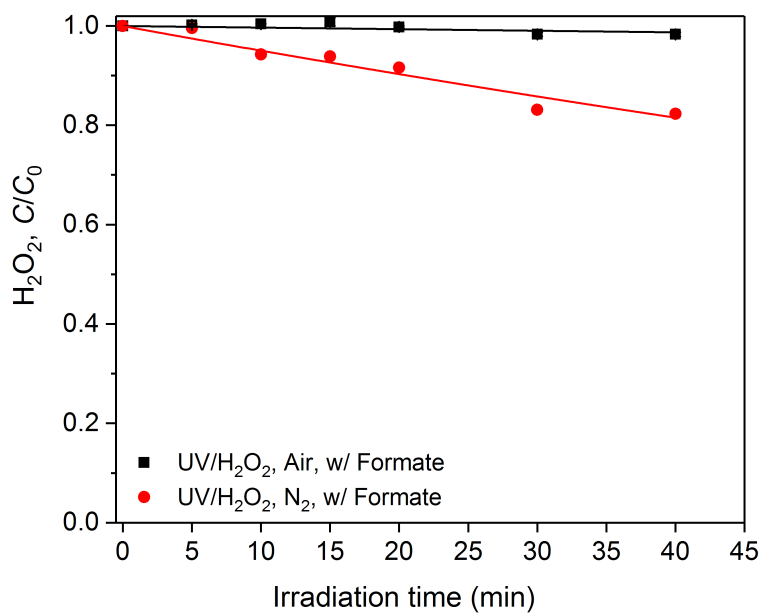


Fig. S9. The decomposition profiles of H₂O₂ (40 μM) in binary mixture with formate (50 μM) at air-saturated or N₂-purged conditions.

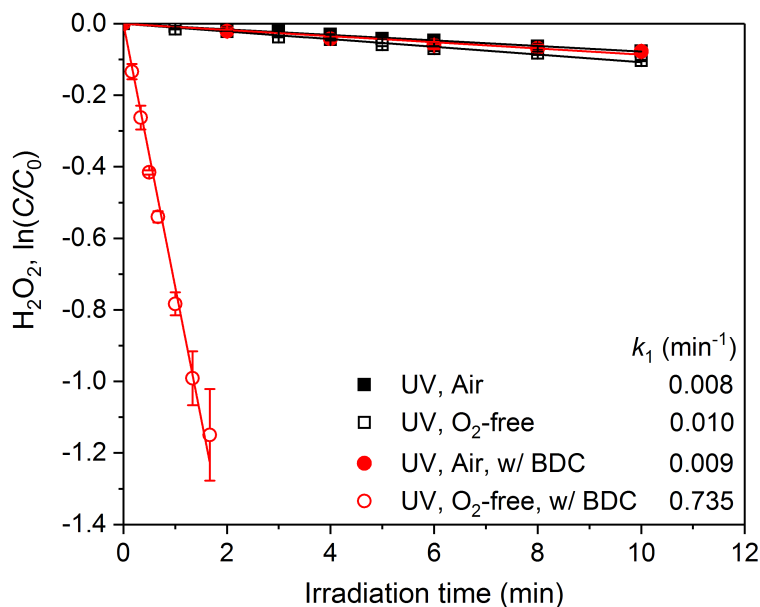


Fig. S10. The decomposition profiles of H_2O_2 ($20 \mu\text{M}$) in H_2O_2 -only or H_2O_2 -BDC ($20 \mu\text{M}$) binary solutions at air-saturated or O_2 -free conditions (pH: 9.0). The concentration of O_2 in this O_2 -free BDC solution was below the detection limit (0.01 mg L^{-1}). The absorbance of the irradiated solution was controlled below 0.35 to ensure that there was a sufficient number of photons.

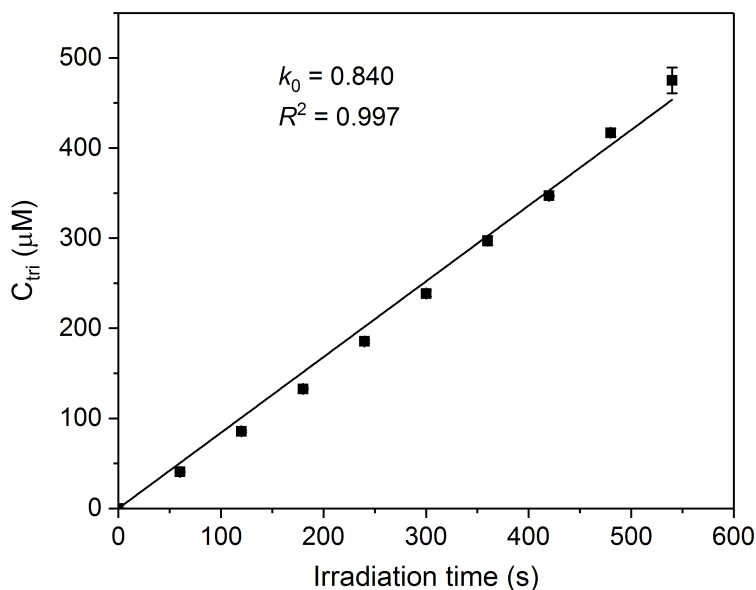


Fig. S11. Formation of I_3^- in a KI/KIO_3 chemical actinometer under 254 nm irradiation. $[\text{KI}]_0$: 0.6 M, $[\text{KIO}_3]_0$: 0.1 M, buffer: 10 mM borate, pH 9.0, 25°C . Error bars indicate the standard deviation of duplicate experiments. Scatter: experimental data, line: linear fitting.

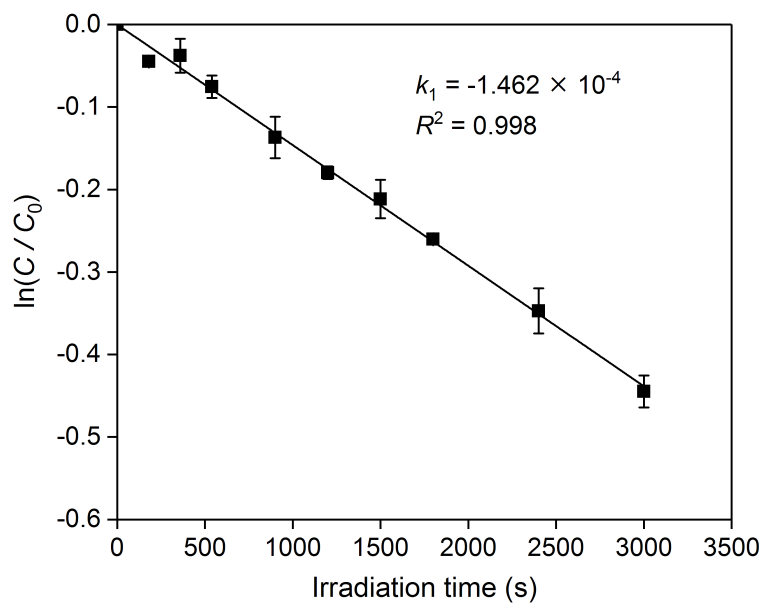


Fig. S12. Photolysis of a H_2O_2 solution ($520 \mu\text{M}$) with the LP-Hg lamp. Scatter: experimental data, line: linear fitting.

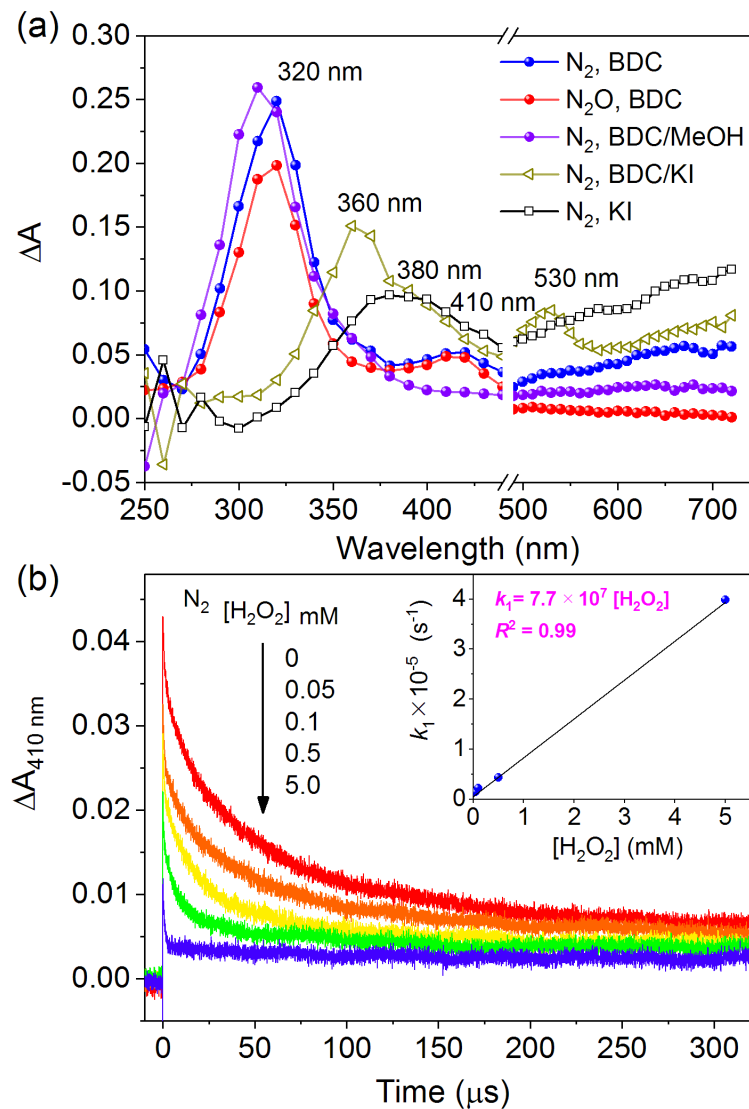


Fig. S13. (a) Transient absorption spectra of BDC at different conditions after laser pulse of 0.2 μs . (b) Decay traces of the 410 nm species. Inset: k_1 of the 410 nm species vs $[H_2O_2]_0$ in N_2 -purged BDC solution. $[BDC]$: 0.1 mM, $[KI]_0$: 0.1 M. MeOH: methanol as the solvent.

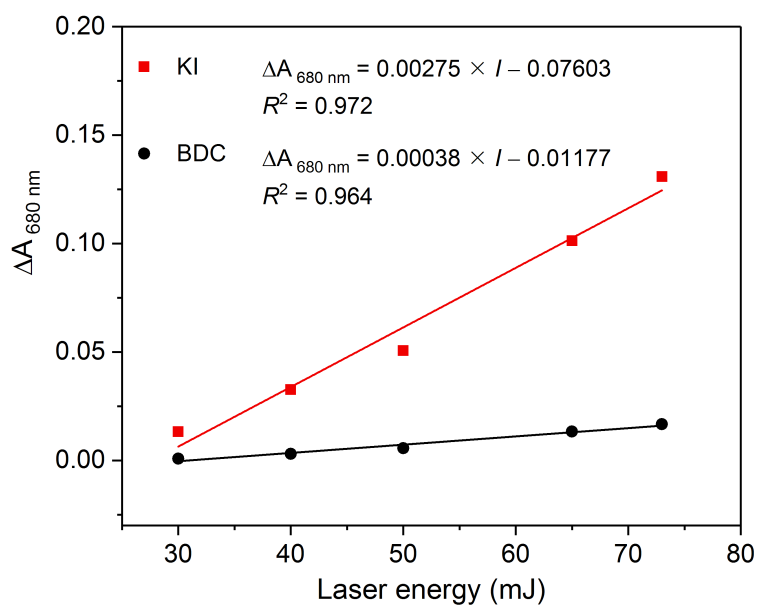
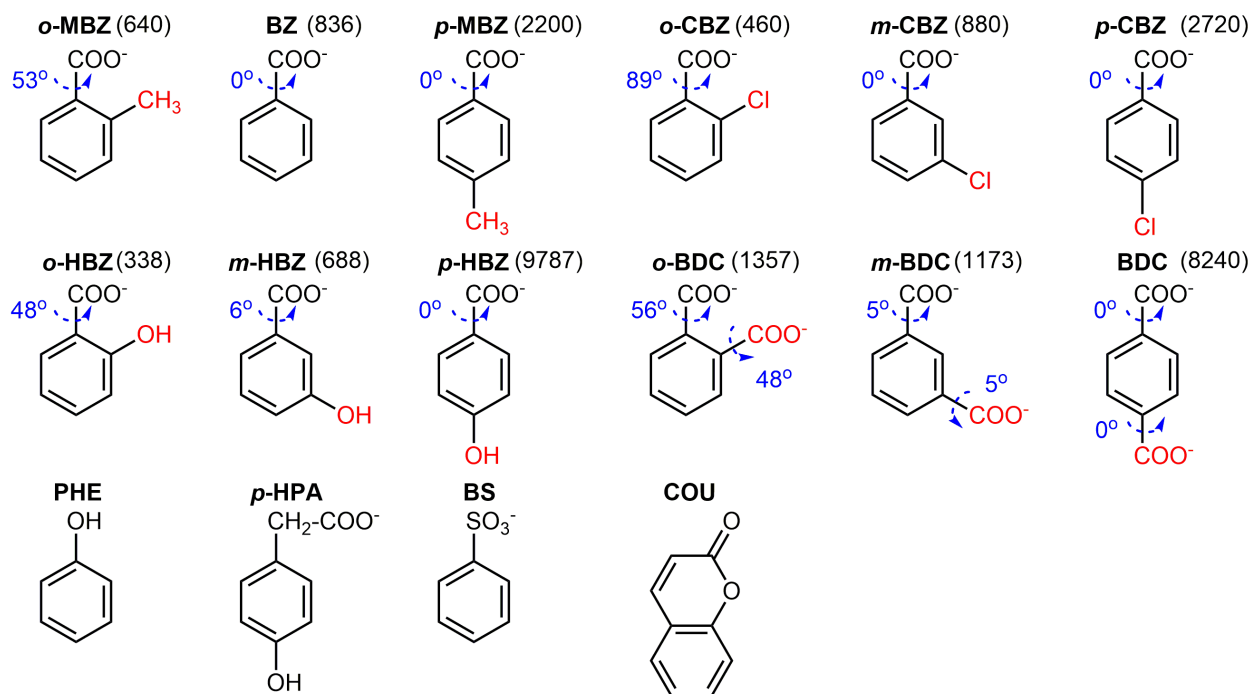
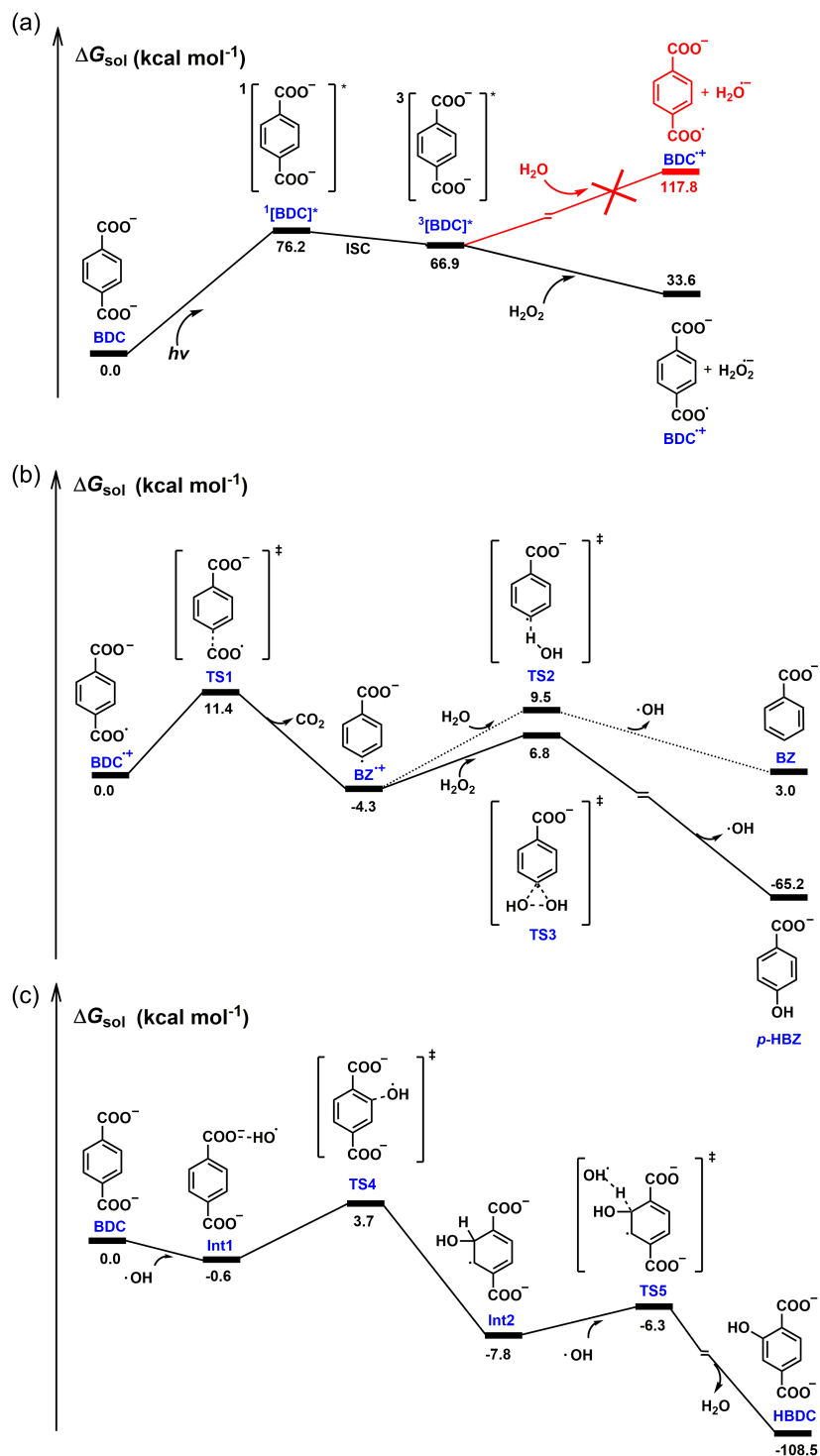


Fig. S14. Dependence of the 680 nm absorbance (immediately after the 266 nm laser pulse of KI and BDC in N₂-purged phosphate buffer solutions) on laser intensity. [BDC]₀: 0.5 mM, [KI]₀: 0.251 M, buffer: 20 mM, pH 7.0.

Chart S1. Structures and abbreviations of the 16 model compounds. The dash arrow represents carbonyl group twists out of the aromatic ring plane due to the substitution, and the near data is dihedral angle. The data in parentheses is molar extinction coefficient at 254 nm ($\epsilon_{254 \text{ nm}}$, in $\text{M}^{-1} \text{cm}^{-1}$).



Scheme S1. (a) The energy level diagram of the UV-induced photochemical process in deoxygenated BDC solution with (black) or without (red) H_2O_2 at 298 K. (b) Free energy profile for the subsequent process after the production of BDC^{++} at 298 K. (c) Free energy profile for the reaction pathway of BDC with $\cdot\text{OH}$ at 298 K.



Scheme S2. The possible reaction pathways of ${}^3\text{BDC}^*$.

